

# Stereoselectivities and Regioselectivities of (4 + 3) Cycloadditions Between Allenamide-Derived Chiral Oxazolidinone-Stabilized Oxyallyls and Furans: Experiment and Theory

Jennifer E. Antoline,<sup>†</sup> Elizabeth H. Krenske,<sup>\*,†,§</sup> Andrew G. Lohse,<sup>†</sup> K. N. Houk,<sup>\*,†</sup> and Richard P. Hsung<sup>\*,†</sup>

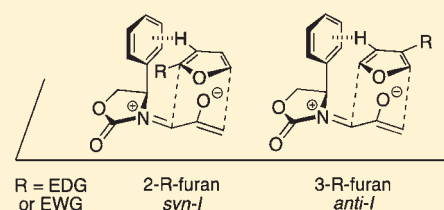
<sup>†</sup>Division of Pharmaceutical Sciences and Department of Chemistry, University of Wisconsin, Madison, Wisconsin 53705, United States

<sup>‡</sup>Department of Chemistry and Biochemistry, University of California, Los Angeles, California 90095, United States

<sup>§</sup>School of Chemistry, University of Melbourne, Victoria 3010, Australia, and Australian Research Council Centre of Excellence for Free Radical Chemistry and Biotechnology

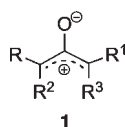
**S** Supporting Information

**ABSTRACT:** A systematic investigation of the regioselectivities and stereoselectivities of (4 + 3) cycloadditions between unsymmetrical furans and a chiral oxazolidinone-substituted oxyallyl is presented. Cycloadditions were performed using an oxyallyl containing a (*R*)-4-phenyl-2-oxazolidinone auxiliary (**2<sub>Ph</sub>**), under either thermal or ZnCl<sub>2</sub>-catalyzed conditions. Reactions of **2<sub>Ph</sub>** with 2-substituted furans gave *syn* cycloadducts selectively, while cycloadditions with 3-substituted furans gave selectively *anti* cycloadducts. The stereoselectivities were in favor of a single diastereoisomer (*I*) in all but one case (2-CO<sub>2</sub>R). Density functional theory calculations were performed to explain the selectivities. The results support a mechanism in which all cycloadducts are formed from the *E* isomer of the oxyallyl (in which the oxazolidinone C=O and oxyallyl oxygen are *anti* to each other) or the corresponding (*E*)-ZnCl<sub>2</sub> complex. The major diastereomer is derived from addition of the furan to the more crowded face of the oxyallyl. Crowded transition states are favored because they possess a stabilizing CH– $\pi$  interaction between the furan and the Ph group.



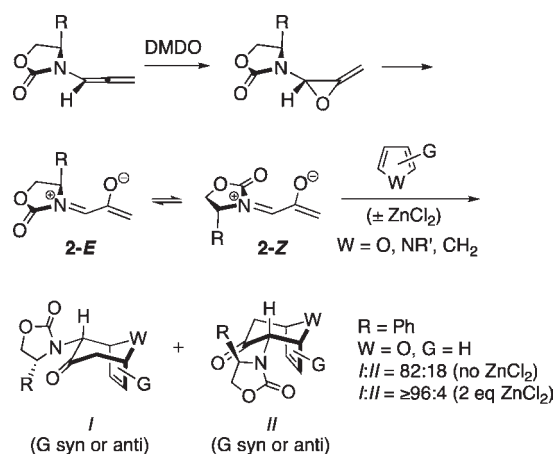
## INTRODUCTION

The (4 + 3) cycloadditions of oxyallyl (**1**) with dienes represent a valuable synthetic route to 7-membered carbocycles.<sup>1</sup> We recently reported the cycloadditions shown in Scheme 1, where a chiral oxazolidinone-stabilized oxyallyl (**2**) is generated by oxidation of an allenamide and reacts with a cyclopentadiene, pyrrole, or furan.<sup>2</sup> This sequence provides access to a diverse range of cycloadducts having *endo* stereochemistry.<sup>3</sup> Regioselective reactions with unsymmetrical furans have also been achieved. During our initial studies, we were surprised to find that the use of a 4-phenyl-2-oxazolidinone auxiliary (**2**, R = Ph) (“**2<sub>Ph</sub>**”) led to unusual selectivities in reactions involving several furans. We have therefore carried out a detailed survey of the regio- and stereochemical features of the oxyallyl protocol using this auxiliary. Experimental and computational results, presented here, support a novel mode of stereoinduction for these reactions, in which the furan adds preferentially to the more crowded face of the oxyallyl. The crowded transition state is stabilized by an attractive CH– $\pi$  interaction between the furan and the Ph group.



Cycloaddition of **2<sub>Ph</sub>** with furan led selectively to the cycloadduct *I* with a diastereomer ratio (*I*:*II*) of 82:18.<sup>2a</sup> In the presence

## Scheme 1. (4 + 3) Cycloadditions of Oxazolidinone-Substituted Oxyallyls



of ZnCl<sub>2</sub>, the dr increased to  $\geq 96:4$ . Originally, it was thought<sup>2</sup> that the stereoselectivities of cycloadditions involving **2** arose through steric control, as depicted in Scheme 2. The presence of the bulky R group was thought to block one face of the oxyallyl from the approaching furan. Addition of the furan to the less

**Received:** June 20, 2011

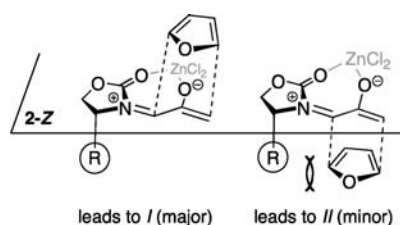
**Published:** August 18, 2011

hindered face of **2-Z** (or its  $\text{ZnCl}_2$  chelate) would lead to the major diastereomer of the cycloadduct (**I**), while addition to the more hindered face would lead to the minor diastereomer (**II**).

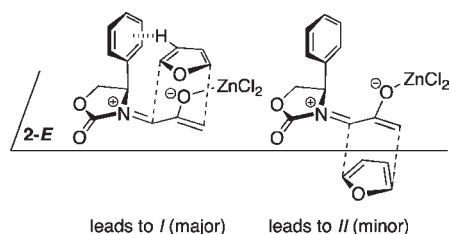
Computational studies, however, revealed an altogether different mechanism.<sup>4</sup> Computations showed that only cycloadditions involving the *E* isomer of **2<sub>Ph</sub>** are energetically feasible (Scheme 3). The O–O repulsion is very destabilizing in conformations previously proposed (Scheme 2). This is true even in the presence of  $\text{ZnCl}_2$ . Furan actually adds to the more crowded face of **2<sub>Ph</sub>-E**, where a favorable  $\text{CH}-\pi$  interaction between the furan and the Ph group stabilizes the transition state by approximately 0.2 kcal/mol over the uncrowded TS.

We present here experimental and computational studies of the cycloadditions of **2<sub>Ph</sub>** with a range of monosubstituted furans, chosen to represent all available variations of electronic character

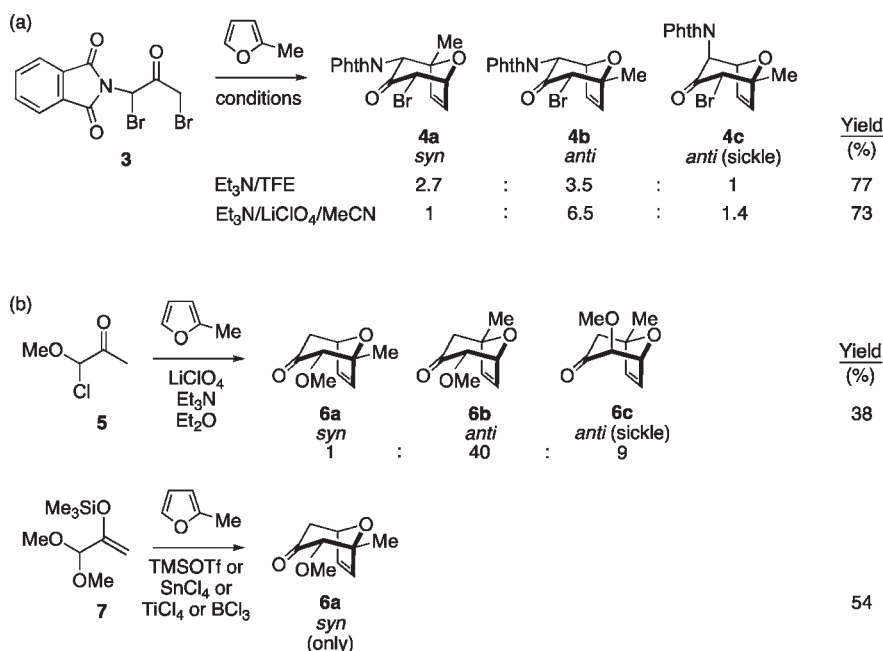
**Scheme 2. Steric Model Originally Proposed for (4 + 3) Cycloadditions of 2**



**Scheme 3. CH– $\pi$ -Directed Stereoinduction**



**Scheme 4. (4 + 3) Cycloadditions of Achiral Oxygen- and Nitrogen-Stabilized Oxallyl Intermediates<sup>5–8</sup>**



and position of substitution. The data support the *anti* disposition of oxygens and attractive  $\text{CH}-\pi$  model and also indicate situations where the  $\text{CH}-\pi$  interaction can be overcome by substituents on the furan, resulting in altered selectivities.

## BACKGROUND

**Previous Reports on Regioselectivities.** Numerous regioselective cycloadditions between furans and N- or O-substituted oxallyls have previously been reported.<sup>1</sup> Some representative examples are shown in Scheme 4. In principle, the reactions of *achiral* heteroatom-substituted oxallyls with unsymmetrical furans can yield two regioisomeric *endo* adducts; we denote these by the terms *syn* and *anti*, in reference to the position ultimately adopted by the substituents on the furan relative to the heteroatom.

Walters<sup>5</sup> generated nitrogen-substituted oxallyl intermediates from the  $\alpha,\alpha'$ -dihalide **3**, by treatment with either  $\text{Et}_3\text{N}$  in trifluoroethanol or  $\text{Et}_3\text{N}/\text{LiClO}_4$  in acetonitrile. Both reacted with 2-methylfuran or 2-methoxyfuran to give predominantly *anti* adducts (**4b**). Föhlisch<sup>6</sup> generated an oxygen-stabilized oxallyl cation by treatment of the  $\alpha$ -halo ketone **5** with  $\text{Et}_3\text{N}/\text{LiClO}_4$ , and its cycloaddition with 2-methylfuran gave predominantly the *anti* cycloadduct **6b**.<sup>7</sup> By contrast, when Albizzati<sup>8</sup> treated the dimethylacetal **7** with a Lewis acid ( $\text{TMSOTf}$ ,  $\text{SnCl}_4$ ,  $\text{TiCl}_4$ , or  $\text{BCl}_3$ ), only the *syn* cycloadduct (**6a**) was obtained. In the reactions of both **3** and **5**, detectable amounts of a third type of adduct resulting from the “sickle” form of the oxallyl intermediate (rather than the “W” form) were also produced.<sup>9</sup>

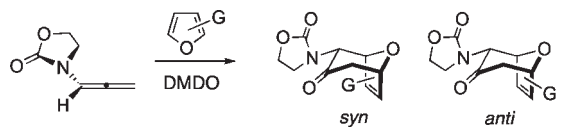
We recently reported the regioselectivities of cycloadditions involving the parent achiral oxazolidinone-substituted oxallyl (Scheme 5).<sup>10</sup> Reactions with 2-methyl- or 2- $\text{CO}_2\text{Me}$ -furan led predominantly to *syn* cycloadducts, while *anti* adducts were obtained from 3-methyl- and 3- $\text{CO}_2\text{Et}$ -furan. Inclusion of  $\text{ZnCl}_2$  increased the yields but had little effect on the regioselectivity.

**Previous Reports on Stereoselectivities.** Incorporation of a chiral auxiliary on the oxallyl increases the number of possible

*endo* cycloadducts to four. For each of the *syn* and *anti* regioisomers, there are two diastereomers, *I* and *II*, which differ according to the face of the oxyallyl intermediate to which the furan binds. Selected literature examples involving chiral nitrogen- and oxygen-substituted oxyallyls are shown in Scheme 6.

Walters generated a chiral nitrogen-stabilized oxyallyl intermediate by treatment of the  $\alpha$ -haloketone **8** with Et<sub>3</sub>N/

**Scheme 5. (4 + 3) Cycloadditions of an Achiral Oxazolidinone-Stabilized Oxyallyl<sup>10</sup>**



G	<i>syn:anti</i>	Yield (%)
2-Me	83:17	90
2-CO <sub>2</sub> Me	≥95:5	41
3-Me	13:87	95
3-CO <sub>2</sub> Et	9:91	36

trifluoroethanol, and it reacted with 3-bromofuran to give selectively the *anti-II* adduct **9**.<sup>11</sup> Hoffmann studied the asymmetric (4 + 3) cycloadditions of oxygen-stabilized oxyallyl cations generated from **10** by treatment with TMSOTf; their cycloadditions with 3-substituted furans led predominantly to *anti-I* adducts.<sup>12</sup> These results have recently been shown to conform to a CH- $\pi$  mode of stereoselection similar to that proposed for our oxyallyls **2**.<sup>13</sup>

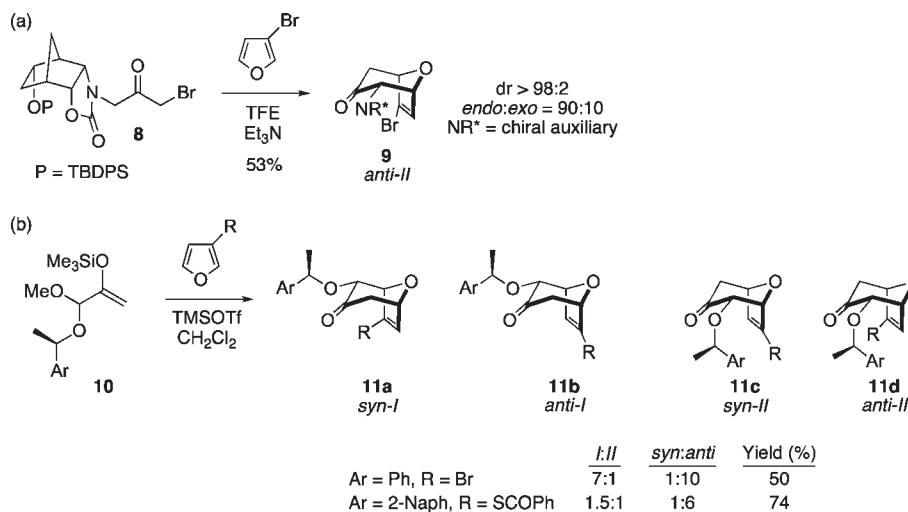
**RESULTS AND DISCUSSION**

We have now investigated the asymmetric cycloadditions of **2**<sub>Ph</sub> with a range of 2- and 3-substituted furans. Methyl and acyloxymethyl-substituted furans were used as electron-rich substrates,<sup>14</sup> while ester and cyano-substituted furans were used as electron-poor substrates. The experimentally measured regio- and stereoselectivities are given in Tables 1–3.<sup>15</sup>

**1. Cycloadditions of **2**<sub>Ph</sub> with 2-Substituted Furans. 1.1.**

*Cycloadditions in the Absence of ZnCl<sub>2</sub>.* The cycloaddition of **2**<sub>Ph</sub> with 2-methylfuran (Table 1) gave a 54% total yield of the *endo* cycloadducts **12a–d**, in which the diastereomer ratio (dr) of *I:II*

**Scheme 6. (4 + 3) Cycloadditions of Chiral Oxygen- and Nitrogen-Stabilized Oxyallyl Intermediates<sup>11,12</sup>**

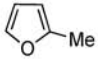
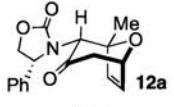
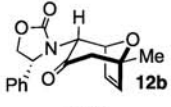
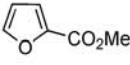
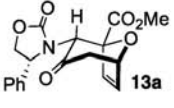
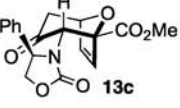
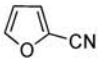
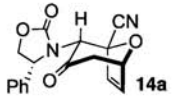
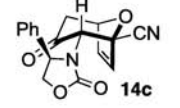


**Table 1. Cycloadditions of **2**<sub>Ph</sub> with 2-Substituted Furans in the Absence of ZnCl<sub>2</sub><sup>a</sup>**

Entry	Furan	<i>syn-endo-I</i>	<i>anti-endo-I</i>	<i>syn-endo-II</i>	<i>anti-endo-II</i>	Yield (%)
1						54
	6–9 equiv	(67)	(23)	(7)	(3)	
2		–	–		–	60
	3 equiv			(100) X-Ray		
3		–	–		–	40
	3 equiv			(100)		

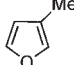
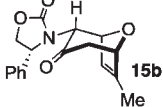
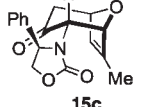
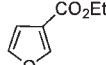
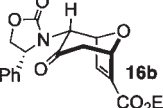
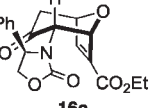
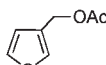
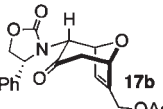
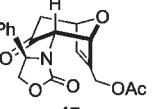
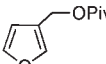
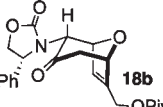
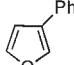
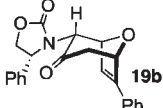
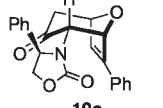
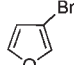
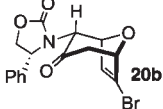
<sup>a</sup> Isolated yields. Isomer distributions are given in parentheses and were determined by <sup>1</sup>H and/or <sup>13</sup>C NMR.

Table 2. Cycloadditions of  $2_{Ph}$  with 2-Substituted Furans in the Presence of  $ZnCl_2^a$ 

Entry	Furan	<i>syn-endo-I</i>	<i>anti-endo-I</i>	<i>syn-endo-II</i>	<i>anti-endo-II</i>	Yield (%)
1		 12a (80)	 12b (20)	–	–	47
	6–9 equiv					
2		 13a (30)	–	 13c (70)	–	63
	3 equiv					
3		 14a (83)	–	 14c (17)	–	47
	3 equiv					

<sup>a</sup> Isolated yields. Isomer distributions are given in parentheses and were determined by <sup>1</sup>H and/or <sup>13</sup>C NMR.

Table 3. Cycloadditions of  $2_{Ph}$  with 3-Substituted Furans in the Presence of  $ZnCl_2^a$ 

Entry	Furan	<i>syn-endo-I</i>	<i>anti-endo-I</i>	<i>syn-endo-II<sup>b</sup></i>	<i>anti-endo-II</i>	Yield (%)
1		–	 15b (88)	 15c (12)	–	62
	6–9 equiv					
2		–	 16b (90) X-Ray	 16c (10)	–	60
	3 equiv					
3		–	 17b (70)	 17c (30)	–	49
	6–9 equiv					
4		–	 18b (100)	–	–	53
	6–9 equiv					
5		–	 19b (60)	 19c (40)	–	50
	6–9 equiv					
6		–	 20b (100) X-Ray	–	–	45
	6–9 equiv					

<sup>a</sup> Isolated yields. Isomer distributions are given in parentheses and were determined by <sup>1</sup>H and/or <sup>13</sup>C NMR. <sup>b</sup> The regiochemistry of all minor isomers were assigned as *syn* by COSY and NMR coupling patterns, but the stereochemistry (*I* or *II*) was not determined; they are listed as *II* here by comparison with the computational data.

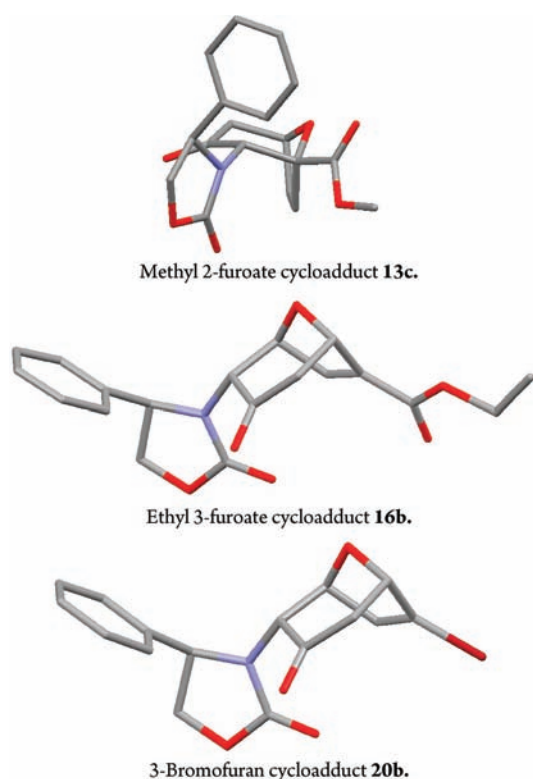


Figure 1. X-ray crystal structures of cycloadducts.

was 90:10. The regioisomer ratios were equivalent for the two diastereomers: *I* was obtained with a *syn:anti* ratio of 67:23 (**12a:12b**), while *II* was obtained with a *syn:anti* ratio of 70:30 (**12c:12d**). Stereochemical assignments were made on the basis of NMR coupling patterns and COSY spectra. The olefinic protons in both of the *I* isomers (**12a** and **12b**) are shifted unusually upfield, due to anisotropic shielding by the nearby Ph ring on the oxazolidinone. Similar shielding effects were also observed with the other *I* isomers described below. The *II* isomers **12c** and **12d** showed no such upfield shifting. For the *syn-I* isomer (**12a**), the  $^1\text{H}$  NMR spectrum had to be collected at high temperature to discern the coupling patterns (Supporting Information).

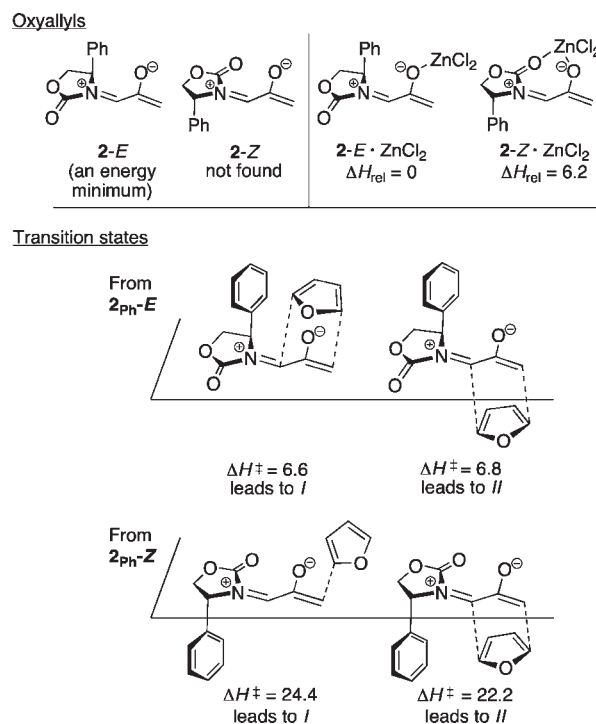
In contrast, the cycloadditions of **2<sub>Ph</sub>** with 2-EWG-substituted furans produced diastereomer *II* but no observable *I*. Methyl 2-furoate and allyl 2-furoate gave the *syn-II* isomers **13c** and **13'c** as the sole cycloadducts in 40–60% yield. The stereochemistry of **13c** was unambiguously assigned by X-ray crystallography (Figure 1).

**1.2. Cycloadditions in the Presence of  $\text{ZnCl}_2$ .** Inclusion of  $\text{ZnCl}_2$  in the reaction mixture for cycloaddition with 2-methylfuran raised the diastereomer ratio from 90:10 to 100:0 (Table 2). The *syn:anti* ratio increased to 80:20.

With methyl 2-furoate, the major product was still the *syn-II* isomer **13c**, but it was now accompanied by a small amount of *syn-I* (**13a**). The structure of **13a** was assigned spectroscopically; anisotropic shielding was again evident.<sup>2d</sup> Somewhat surprisingly, on going from the furoate ester to its nitrile analogue, a return in stereoselectivity back to *I* was observed! The *syn-I* isomer **14a** was obtained from 2-cyanofuran with a dr of 83:17. The regioselectivity for both the ester and the nitrile was completely in favor of *syn*.

The regioselectivities observed here parallel those observed previously for the parent oxazolidinone-substituted oxyallyl

**Scheme 7. Previous Calculations<sup>4</sup> on the Oxyallyl **2<sub>Ph</sub>**, its  $\text{ZnCl}_2$  Complexes, and its Cycloadditions with Furan. Energies are in kcal/mol**



(Scheme 5),<sup>10</sup> although for 2-methylfuran the *syn:anti* ratio is lower with **2<sub>Ph</sub>** than with the parent oxyallyl.

**2. Cycloadditions of **2<sub>Ph</sub>** with 3-Substituted Furans.** The cycloadditions of **2<sub>Ph</sub>** with 3-substituted furans were studied under  $\text{ZnCl}_2$ -catalyzed conditions. Our results are listed in Table 3. The stereochemistry of the major cycloadducts was unambiguously assigned by means of COSY and NOESY analysis and, in the cases of ethyl 3-furoate and 3-bromofuran, by X-ray single crystal structures (Figure 1). In all of the major products, the olefinic proton showed the typical anisotropic shielding by the Ph ring on the oxazolidinone. For the minor isomers, the regiochemistry could be firmly assigned as *syn* by COSY and NMR coupling patterns, but the stereochemistry was not determined. The *syn* regiochemistry ruled out the use of Ph shielding as a stereochemical diagnostic. We have tentatively assigned the *II* stereochemistry to the minor isomers, on the basis of our computational results reported below.

The regio- and stereoselectivities of the cycloadditions involving 3-substituted furans differ markedly from those of 2-substituted furans. All of the 3-substituted furans gave selectively the *anti-I* cycloadduct. For 3-methylfuran and methyl 3-furoate, the *anti:syn* ratio was approximately 90:10. 3-phenylfuran and 3-acetoxymethylfuran gave more modest *anti:syn* ratios (60:40 and 70:30, respectively), but replacement of the acetyl group in the latter by a pivaloyl group increased the *anti* selectivity to 100:0. 3-bromofuran also gave 100:0 *anti* selectivity.

The regioselectivities of these reactions mirror those of the parent oxazolidinone-substituted oxyallyl with 3-substituted furans (Scheme 5),<sup>10</sup> both in direction and magnitude. Similar *anti-I* selectivity was reported by Hoffmann for the cycloadditions of 3-substituted furans with related oxygen-substituted oxyallyl cations (Scheme 6).<sup>12</sup>



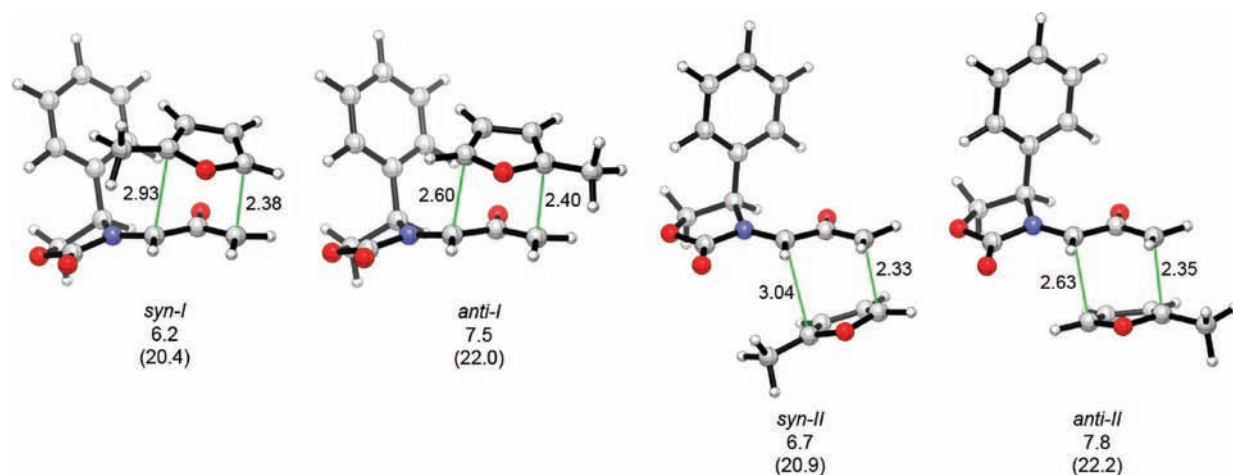


**Figure 2.** Transition structures for the (4 + 3) cycloadditions of  $2_{Ph}$  with 2-methylfuran, calculated at the B3LYP/6-31G(d) level. Bond lengths in Å, energies in kcal/mol.  $\Delta H^\ddagger$  and  $\Delta G^\ddagger$  (in parentheses) are given below the TSs.

**Table 4. Calculated Activation Energies and Experimental Cycloadduct Ratios for the (4 + 3) Cycloadditions of  $2_{Ph}$  with 2-Substituted Furans<sup>a</sup>**

	<i>syn-I</i>	<i>anti-I</i>	<i>syn-II</i>	<i>anti-II</i>
Reactions in the absence of $ZnCl_2$				
2-Methylfuran				
$\Delta H^\ddagger$	6.2	7.5	6.7	7.8
$\Delta G^\ddagger$	20.4	22.0	20.9	22.2
Experimental	67%	23%	7%	3%
Methyl 2-furoate				
$\Delta H^\ddagger$	5.3	8.7	3.4	9.3
$\Delta G^\ddagger$	20.5	23.2	19.3	23.3
Experimental			100%	
Reactions in the presence of $ZnCl_2$				
2-Methylfuran				
$\Delta H^\ddagger$	-2.9	-1.7	-1.9	-0.6
$\Delta G^\ddagger$	11.7	13.6	11.7	13.4
Experimental	80%	20%		
Methyl 2-furoate				
$\Delta H^\ddagger$	-1.1	4.1	-1.7	5.4
$\Delta G^\ddagger$	14.1	18.5	13.9	18.4
Experimental	30%		70%	
2-Cyanofuran				
$\Delta H^\ddagger$	2.3	6.1	3.4	7.6
$\Delta G^\ddagger$	17.0	20.9	17.7	21.4
Experimental	83%		17%	

<sup>a</sup> B3LYP/6-31G(d), 298.15 K, kcal/mol; Experimental isomer ratios given as percentages.

**3. Computational Studies.** Numerous theoretical studies of oxyallyl cations and their cycloadditions have been reported previously.<sup>5,16–18</sup> Cramer<sup>17b,c</sup> showed that the cycloadditions can take place by various mechanisms; the highly electrophilic hydroxyallyl cation was calculated to react with furan by a two-step process commencing with electrophilic attack at C-2 of the furan. We have found<sup>4</sup> that the less electrophilic, neutral oxyallyls **2** undergo concerted, asynchronous cycloadditions with furans.

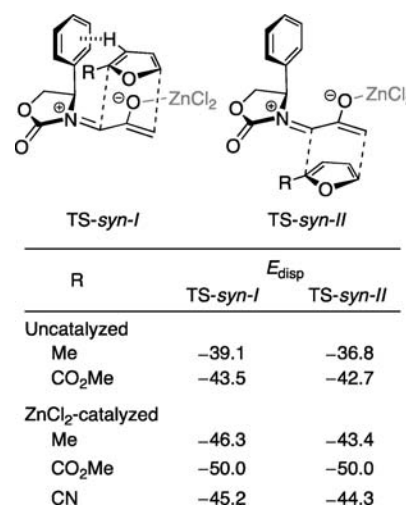


**Figure 3.** Total dispersion energies of the *syn-I* and *syn-II* transition states for cycloadditions of  $2_{Ph}$  with 2-substituted furans, calculated at the B3LYP-D/6-31G(d) level (kcal/mol).

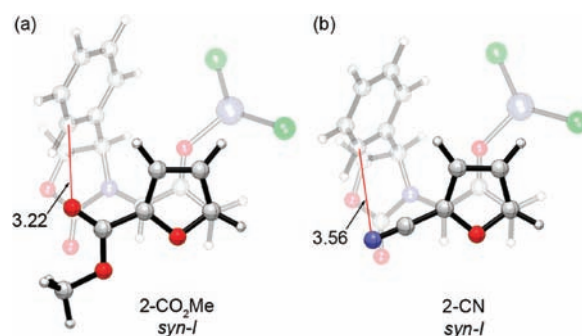


**Figure 4.** *Syn-I* transition structures for the  $ZnCl_2$ -catalyzed (4 + 3) cycloadditions of  $2_{Ph}$  with 2-CO<sub>2</sub>Me- and 2-CN-furan, calculated at the B3LYP/6-31G(d) level. Distances in Å.

Our earlier findings<sup>4</sup> are summarized in Scheme 7. At the B3LYP/6-31G(d) level, only the *E* conformer of  $2_{Ph}$  was an energy minimum. Attempts to locate the *Z* conformer led to the

**Table 5. Calculated Activation Energies and Experimental Cycloadduct Ratios for the ZnCl<sub>2</sub>-Catalyzed (4 + 3) Cycloadditions of 2<sub>Ph</sub> with 3-Substituted Furans<sup>a</sup>**

	<i>syn-I</i>	<i>anti-I</i>	<i>syn-II</i>	<i>anti-II</i>
3-Methylfuran				
$\Delta H^\ddagger$	-1.4	-2.8	-2.0	-1.9
$\Delta G^\ddagger$	12.7	11.6	11.8	10.9
Experimental		88%	12%	
Methyl 3-furoate				
$\Delta H^\ddagger$	0.9	-4.9	-1.9	-3.2
$\Delta G^\ddagger$	16.7	11.7	13.2	12.8
Experimental <sup>b</sup>		90%	10%	

<sup>a</sup> B3LYP/6-31G(d), 298.15 K, kcal/mol; experimental isomer ratios given as percentages. <sup>b</sup> Experimental data for ethyl 3-furoate.

isomeric cyclopropanone. ZnCl<sub>2</sub> complexes were located for both the *E* and the *Z* conformers, but the *Z* complex was 6.2 kcal/mol less stable. Transition states were located for cycloadditions involving both the *E* and the *Z* conformers, but those involving the *Z* isomer were disfavored by  $\geq 15.4$  kcal/mol ( $\geq 5.2$  kcal/mol for the ZnCl<sub>2</sub> complexes). Electrostatic repulsion between the oxygen atoms destabilizes all of the *Z* structures.

The concerted transition state geometries are asynchronous such that the more advanced bonding interaction involves the more nucleophilic (CH<sub>2</sub>) carbon of the oxyallyl. This is the case also for reactions with substituted furans, shown in Scheme 5.<sup>10</sup> On the other hand, the calculated Mulliken charges in the transition states indicate net charge transfer of 0.05–0.17e from the furan to the oxyallyl. Overall, the oxyallyls **2** are best characterized as ambiphilic toward furans. The activation barriers for reactions with either Me- or CO<sub>2</sub>Me-substituted furans (Scheme 5) are lower than those for furan itself. Methyl 2-furoate has the lowest barrier ( $\Delta H^\ddagger$  3.2 kcal/mol lower than for furan).

To model the reactions of 2<sub>Ph</sub> with substituted furans, we calculated transition states involving addition to the *E* oxyallyl only. Calculations were performed at the B3LYP/6-31G(d) level (including LANL2DZ+ECP for Zn) in Gaussian 03.<sup>19</sup> In Figure 2 are shown the four isomeric transition structures calculated for the reaction of 2<sub>Ph</sub> with 2-methylfuran. These are representative of the transition states calculated for the other furans also. Concerted, asynchronous transition states were found for all of the cycloadditions.

**3.1. Cycloadditions of 2<sub>Ph</sub> with 2-Substituted Furans.** The calculated activation energies for reactions of 2<sub>Ph</sub>-*E* with 2-substituted furans are listed in Table 4. The experimental selectivities are also included in the table for comparison.

The calculations correctly predict the major product for each 2-substituted furan. Some differences in the minor isomers are found, which for the ZnCl<sub>2</sub>-catalyzed cycloadditions may be due to the use of excess furan and ZnCl<sub>2</sub> in the experiment. For example, a furan molecule may coordinate to the Zn center of 2<sub>Ph</sub>-*E*·ZnCl<sub>2</sub>, or ZnCl<sub>2</sub> may coordinate to the furan that undergoes cycloaddition. These factors would lead to small differences in the proportions of the minor isomers but are unlikely to affect the overall selectivity.

The oxyallyl 2<sub>Ph</sub> is more nucleophilic at the CH<sub>2</sub> terminus and more electrophilic at the CHN terminus. Yet, cycloadditions of 2<sub>Ph</sub> with both 2-EWG and 2-EDG-substituted furans favor the *syn* cycloadducts. This regioselectivity is predictable for the EWG-substituted furans, since the substituent renders the

5-position of the furan more electrophilic than the 2-position. The regioselectivity for the donor-substituted furan (2-Me-furan) is unexpected. Here electronic effects are small, and the regioselectivity instead arises from a preference for the transition state that allows the more advanced bonding interaction to be made to the less-substituted carbon (C-5) of the furan (Figure 2).

The stereoselectivities observed with 2-methylfuran and 2-cyanofuran conform to the CH- $\pi$  model (Scheme 3) and have a magnitude somewhat smaller than that observed with furan itself (82:18 uncatalyzed,  $\geq 96:4$  with ZnCl<sub>2</sub>). The proton involved in the CH- $\pi$  interaction is H-3 or H-4 of the furan (for the *syn* and *anti* isomers, respectively), which points roughly toward the center of the Ph ring in the *I* transition states. The stabilizing role of the CH- $\pi$  interaction has both electrostatic and dispersive components. To estimate the role of the latter, the dispersion energies in the transition states were calculated by means of Grimme's 2006 empirical B3LYP-D formula, which sums the dispersion energies between each pair of atoms in the structure.<sup>20</sup> A comparison between the dispersion energies of the *syn-I* and *syn-II* transition states for each 2-substituted furan is shown in Figure 3. Dispersive stabilization is 0.02–2.9 kcal/mol stronger in the *I* transition states than the *II* transition states.

The reversal in stereoselectivity for 2-CO<sub>2</sub>Me-furan was at first surprising, but it is indeed predicted by theory. The *syn-II* transition state is favored over the other three TSs by 1.9 kcal/mol in the uncatalyzed reaction and by 0.6 kcal/mol in the ZnCl<sub>2</sub>-catalyzed reaction ( $\Delta\Delta H^\ddagger$ ). A top-down view of the *syn-I* transition state for 2-CO<sub>2</sub>Me-furan under ZnCl<sub>2</sub>-catalyzed conditions is shown in Figure 4a. A destabilizing electrostatic interaction takes place between the ester carbonyl group and the Ph  $\pi$ -cloud. The distance between the carbonyl oxygen and the nearby C-2 of the Ph ring (red line: 3.22 Å) is equal to the sum of the van der Waals radii for C and O. This interaction outweighs the stabilizing effect of the CH- $\pi$  interaction, and the uncrowded (*II*) transition state is instead favored.

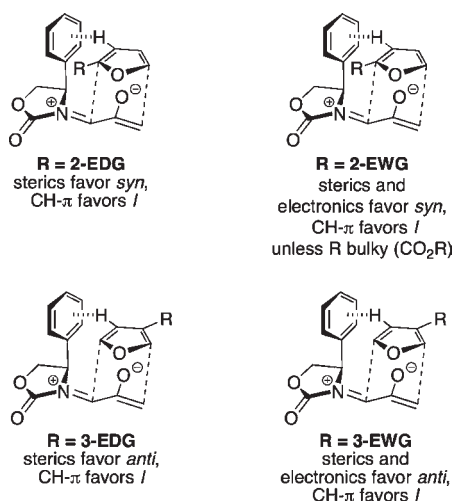
The calculations also correctly predict that the seemingly small change from a 2-CO<sub>2</sub>Me to a 2-CN group should induce a return to *syn-I* selectivity. The *syn-I* transition state for 2-CN-furan is shown in Figure 4b. The CN group is positioned further from the Ph ring (N–C 3.56 Å), and therefore does not present such severe electrostatic repulsion as the CO<sub>2</sub>Me group.

**3.2. Cycloadditions of 2<sub>Ph</sub> with 3-Substituted Furans.** The calculated activation energies for ZnCl<sub>2</sub>-catalyzed reactions of 2<sub>Ph</sub> with 3-substituted furans are listed in Table 5, together with the experimental selectivities.

The calculations correctly predict the regio- and stereochemistry of the major product for methyl 3-furoate. For 3-methylfuran, the free energies of activation do not capture the correct stereoselectivity, but the enthalpies do predict both the regio- and stereoselectivity. As with the 2-EWG-substituted furans, the regioselectivity for 3-CO<sub>2</sub>Me-furan is under electronic control, since C-2 of the furan is more electrophilic than C-5. For 3-Me-furan, the regioselectivity is instead steric in origin, arising through avoidance of clashing between the Me group and the Ph group.

Both 3-substituted furans favor the *I* stereoisomer, as do the four other 3-substituted furans in Table 3. The *anti* arrangement enables the CH- $\pi$  interaction in the crowded TS to take place without interference from the substituent. The calculations predict that for both 3-substituted furans, the minor (*syn*) isomer

### Scheme 8. Summary of Factors Responsible for Regio- and Stereocontrol in the (4 + 3) Cycloadditions of **2**<sub>Ph</sub> with Furans



should have the *II* stereochemistry, as the *syn-I* transition state is subject to unfavorable interaction between the Ph group and the furan 3-substituent.

### CONCLUSIONS

A summary of the origins of the regio- and stereoselectivities of the (4 + 3) cycloadditions is given in Scheme 8. The oxyallyls **2** undergo (4 + 3) cycloadditions with furans through concerted transition states in most cases. Generally, bond development at the TS is most advanced at the nucleophilic (CH<sub>2</sub>) terminus of **2**. The regioselectivities of (4 + 3) cycloadditions between **2** and furans arise through steric effects, but these are complemented by electronic effects when the substituent is an electron-withdrawing group. For 2-substituted furans, *syn* cycloadducts are formed selectively, because this arrangement enables the stronger bonding interaction in the TS to involve the less-hindered (C-5) carbon. For 2-EWG-substituted furans, C-5 is also more electrophilic than C-2, enhancing regiocontrol. 3-Substituted furans undergo cycloaddition preferentially in the *anti* geometry, in order to avoid steric clashing between the 3-substituent and the Ph ring. Similar *anti* selectivity has even been observed when the Ph group is absent,<sup>10</sup> indicating that the pseudoaxial group at the 4-position of the oxazolidinone has a steric influence even when it is only an H atom. For 3-EWG-substituted furans, the *anti* selectivity is complemented by the electronic effect of the substituent, which renders C-2 more electrophilic than C-5.

All but two of the furans studied (Tables 1–3) lead selectively to the cycloadduct *I*. Only for 2-CO<sub>2</sub>R-furans (R = Me, allyl) does the unexpected *II* isomer predominate. The CH- $\pi$  model (Scheme 3) therefore appears to have broad applicability for monosubstituted furans. When the oxazolidinone Ph group is replaced by a nonaromatic group, the stabilizing CH- $\pi$  interaction is lost, and the stereoselectivity reverts to favor *II*, as shown by our earlier studies with a 4-Bn-oxazolidinone and with Seebach et al.'s<sup>21</sup> 4-<sup>t</sup>Pr-5,5-Ph<sub>2</sub>-oxazolidinone auxiliary.<sup>4</sup> Reversals of stereoselectivity have also previously been observed to occur in hetero-Diels–Alder reactions<sup>22</sup> and conjugate radical additions<sup>23</sup> catalyzed by chiral Lewis acid/bis(oxazoline) complexes, when the Ph groups on the ligand were replaced by <sup>t</sup>Bu groups.

Chiral oxazolidinone auxiliaries have been used to achieve a wide range of other asymmetric transformations, including Diels–Alder reactions,<sup>24</sup> aldol condensations,<sup>25</sup> enolate alkylation,<sup>26</sup> hydroxylation,<sup>27</sup> and amination,<sup>28</sup> Michael additions,<sup>29</sup> epoxide synthesis,<sup>30</sup> and resolutions of  $\alpha$ -halo carbonyl compounds.<sup>31</sup> The results described herein for the (4 + 3) cycloadditions of **2**<sub>Ph</sub> likely hold relevance to stereocontrol in these other oxazolidinone-directed reactions.

### EXPERIMENTAL METHODS

**Typical Procedure for (4 + 3) Cycloadditions.** To a solution of the allenamide in CH<sub>2</sub>Cl<sub>2</sub> (0.1 M) were added the appropriate furan (3–9 equiv) and 4 Å powder molecular sieves (0.5 g). The solution was cooled to –78 °C, and ZnCl<sub>2</sub> (1.0 M in ether, 2.0 equiv) was added. DMDO (4.0–6.0 equiv, in acetone) was then added as a chilled solution via syringe pump (at –78 °C) over 3–4 h. The reaction mixture was stirred for a further 14 h, then quenched with saturated aqueous NaHCO<sub>3</sub>, filtered through Celite, concentrated *in vacuo*, extracted with CH<sub>2</sub>Cl<sub>2</sub>, dried over Na<sub>2</sub>SO<sub>4</sub>, and concentrated *in vacuo*. The crude residue was purified via column chromatography on silica gel (gradient eluent: 10 to 75% ethyl acetate in hexane).

### THEORETICAL CALCULATIONS

Density functional theory calculations were performed at the B3LYP/6-31G(d) level<sup>32</sup> in Gaussian 03.<sup>19</sup> The LANL2DZ basis set and effective core potential were used for Zn.<sup>33</sup> Species were characterized as minima or transition states on the basis of vibrational frequency analysis and, where appropriate, IRC calculations.<sup>34</sup> Zero-point energy and thermal corrections were derived (unscaled) from the B3LYP/6-31G(d) frequencies. Conformational searching was performed for each species in order to identify the lowest-energy conformer. Enthalpies and free energies are reported at 298.15 K, with a standard state of 1 atm.

### ASSOCIATED CONTENT

**S Supporting Information.** Full experimental procedures, NMR spectra and characterizations for all new compounds, X-ray data, computed geometries and energies, and a complete citation for ref 19. This material is available free of charge via the Internet at <http://pubs.acs.org>.

### AUTHOR INFORMATION

#### Corresponding Author

ekrenske@unimelb.edu.au; houk@chem.ucla.edu; rhsung@wisc.edu

### ACKNOWLEDGMENT

We thank the NIH (GM36700 to KNH and GM-66055 to R. P.H.) and Australian Research Council (DP0985623 to E.H.K.) for generous financial support, and the NCSA, UCLA ATS, UCLA IDRE, and NCF NI (Australia) for computer resources. EHK also thanks the Australian–American Fulbright Commission for a postdoctoral scholarship and the ARC Centre of Excellence for Free Radical Chemistry and Biotechnology for financial support. We thank Dr Vic Young and Dr Ben Kucera of the University of Minnesota for X-ray crystallography.

### REFERENCES

- (1) For reviews, see: (a) Lohse, A. G.; Hsung, R. P. *Chem.—Eur. J.* **2011**, *17*, 3812–3822. (b) Harmata, M. *Chem. Commun.* **2010**, *46*, 8886–8903. (c) Harmata, M. *Adv. Synth. Catal.* **2006**, *348*, 2297–2306.



- (d) Battiste, M. A.; Pelphey, P. M.; Wright, D. L. *Chem.—Eur. J.* **2006**, *12*, 3438–3447. (e) Antoline, J. E.; Hsung, R. P. *ChemTracts* **2005**, *18*, 562–568. (f) Hartung, I. V.; Hoffmann, H. M. R. *Angew. Chem., Int. Ed.* **2004**, *43*, 1934–1949. (g) Harmata, M.; Rashatasakhon, P. *Tetrahedron* **2003**, *59*, 2371–2395. (h) Harmata, M. *Acc. Chem. Res.* **2001**, *34*, 595–605. (i) Davies, H. M. L. In *Advances in Cycloaddition*; Harmata, M., Ed.; JAI: Stamford, CT, 1999; Vol. 5, 119–164. (j) West, F. G. In *Advances in Cycloaddition*; Lautens, M., Ed.; JAI: Greenwich, CT, 1997; Vol. 4, 1–40. (k) Rigby, J. H.; Pigge, F. C. *Org. React.* **1997**, *51*, 351–478. (l) Harmata, M. *Tetrahedron* **1997**, *53*, 6235–6280. (m) Harmata, M. *Recent Res. Devel. Org. Chem.* **1997**, *1*, 523–535. (n) Katritzky, A. R.; Dennis, N. *Chem. Rev.* **1989**, *89*, 827–861.
- (2) (a) Xiong, H.; Hsung, R. P.; Berry, C. R.; Rameshkumar, C. *J. Am. Chem. Soc.* **2001**, *123*, 7174–7175. (b) Rameshkumar, C.; Xiong, H.; Tracey, M. R.; Berry, C. R.; Yao, L. J.; Hsung, R. P. *J. Org. Chem.* **2002**, *67*, 1339–1345. (c) Xiong, H.; Huang, J.; Ghosh, S. K.; Hsung, R. P. *J. Am. Chem. Soc.* **2003**, *125*, 12694–12695. (d) Rameshkumar, C.; Hsung, R. P. *Angew. Chem., Int. Ed.* **2004**, *43*, 615–618. (e) Antoline, J. E.; Hsung, R. P.; Huang, J.; Song, Z.; Li, G. *Org. Lett.* **2007**, *9*, 1275–1278. (f) Antoline, J. E.; Hsung, R. P. *Synlett* **2008**, 739–744.
- (3) We use the term “endo” in reference to the relationship between the diene unit and the oxyallyl oxygen in the cycloadducts and the TSs leading to them. Hoffmann has used the term “compact” to describe the same geometry; Hoffmann, H. M. R. *Angew. Chem., Int. Ed.* **1973**, *12*, 819–835.
- (4) Krenske, E. H.; Houk, K. N.; Lohse, A. G.; Antoline, J. E.; Hsung, R. P. *Chem. Sci.* **2010**, *1*, 387–392.
- (5) (a) Walters, M. A.; Arcand, H. R.; Lawrie, D. J. *Tetrahedron Lett.* **1995**, *36*, 23–26. (b) Walters, M. A.; Arcand, H. R. *J. Org. Chem.* **1996**, *61*, 1478–1486.
- (6) Föhlisch, B.; Krimmer, D.; Gehrlach, E.; Käshammer, D. *Chem. Ber.* **1988**, *121*, 1585–1594.
- (7) For related work, see: Harmata, M.; Rashatasakhon, P. *Synlett* **2000**, 1419–1422.
- (8) Murray, D. H.; Albizati, K. F. *Tetrahedron Lett.* **1990**, *31*, 4109–4112.
- (9) “W” and “sickle” oxyallyl configurations are defined in ref 3.
- (10) Lohse, A. G.; Krenske, E. H.; Antoline, J. E.; Houk, K. N.; Hsung, R. P. *Org. Lett.* **2010**, *12*, 5506–5509.
- (11) MaGee, D. I.; Godineau, E.; Thornton, P. D.; Walters, M. A.; Sponholtz, D. J. *Eur. J. Org. Chem.* **2006**, 3667–3680.
- (12) Beck, H.; Stark, C. B. W.; Hoffmann, H. M. R. *Org. Lett.* **2000**, *2*, 883–886.
- (13) Krenske, E. H.; Houk, K. N.; Harmata, M. *Org. Lett.* **2010**, *12*, 444–447.
- (14) Attempts to perform the cycloadditions with more electron-rich furans such as 2-methoxyfuran were hampered by competing oxidation of the furan; see ref 2f.
- (15) Several earlier results on cycloadditions involving 2-substituted furans under other conditions have previously been reported; see ref 2.
- (16) (a) Coolidge, M. B.; Yamashita, K.; Morokuma, K.; Borden, W. T. *J. Am. Chem. Soc.* **1990**, *112*, 1751–1754. (b) Ichimura, A. S.; Lahti, P. M.; Matlin, A. R. *J. Am. Chem. Soc.* **1990**, *112*, 2868–2875. (c) Janoschek, R.; Kalcher, J. *Int. J. Quantum Chem.* **1990**, *38*, 653–664. (d) Turecek, F.; Drinkwater, D. E.; McLafferty, F. W. *J. Am. Chem. Soc.* **1991**, *113*, 5950–5958. (e) Lim, D.; Hrovat, D. A.; Borden, W. T.; Jorgensen, W. L. *J. Am. Chem. Soc.* **1994**, *116*, 3494–3499. (f) Goodman, J. M.; Hoffmann, H. M. R.; Vinter, J. G. *Tetrahedron Lett.* **1995**, *36*, 7757–7760. (g) Ichino, T.; Villano, S. M.; Gianola, A. J.; Goebbert, D. J.; Velarde, L.; Sanov, A.; Blanksby, S. J.; Zhou, X.; Hrovat, D. A.; Borden, W. T.; Lineberger, W. C. *Angew. Chem., Int. Ed.* **2009**, *48*, 8509–8511. (h) Kuzmanich, G.; Spänig, F.; Tsai, C.-K.; Um, J. M.; Hoekstra, R. M.; Houk, K. N.; Guldi, D. M.; Garcia-Garibay, M. A. *J. Am. Chem. Soc.* **2011**, *133*, 2342–2345.
- (17) (a) Noyori, R.; Shimizu, F.; Fukuta, K.; Takaya, H.; Hayakawa, Y. *J. Am. Chem. Soc.* **1977**, *99*, 5196–5198. (b) Cramer, C. J.; Barrows, S. E. *J. Org. Chem.* **1998**, *63*, 5523–5532. (c) Cramer, C. J.; Barrows, S. E. *J. Phys. Org. Chem.* **2000**, *13*, 176–186. (d) Cramer, C. J.; Harmata, M.; Rashatasakhon, P. *J. Org. Chem.* **2001**, *66*, 5641–5644. (e) Harmata, M.; Schreiner, P. R. *Org. Lett.* **2001**, *3*, 3663–3665. (f) Sáez, J. A.; Arnó, M.; Domingo, L. R. *Org. Lett.* **2003**, *5*, 4117–4120. (g) Arnó, M.; Picher, M. T.; Domingo, L. R.; Andrés, J. *Chem.—Eur. J.* **2004**, *10*, 4742–4749. (h) Sáez, J. A.; Arnó, M.; Domingo, L. R. *Tetrahedron* **2005**, *61*, 7538–7545.
- (18) Fernández, I.; Cossío, F. P.; de Cózar, A.; Lledós, A.; Mascareñas, J. L. *Chem.—Eur. J.* **2010**, *16*, 12147–12157.
- (19) Frisch, M. J. et al. *Gaussian 03*, Revision E.01; Gaussian, Inc.: Wallingford, CT, 2004.
- (20) Grimme, S. *J. Comput. Chem.* **2006**, *27*, 1787–1799.
- (21) (a) Hintermann, T.; Seebach, D. *Helv. Chim. Acta* **1998**, *81*, 2093–2126. (b) Gaul, C.; Schweizer, B. W.; Seiler, P.; Seebach, D. *Helv. Chim. Acta* **2002**, *85*, 1546–1566.
- (22) (a) Yao, S.; Johannsen, M.; Audrain, H.; Hazell, R. G.; Jørgensen, K. A. *J. Am. Chem. Soc.* **1998**, *120*, 8599–8605. (b) Evans, D. A.; Johnson, J. S.; Olhava, E. J. *J. Am. Chem. Soc.* **2000**, *122*, 1635–1649.
- (23) Sibi, M. P.; Ji, J.; Hongliu Wu, J.; Gürtler, S.; Porter, N. A. *J. Am. Chem. Soc.* **1996**, *118*, 9200–9201.
- (24) (a) Evans, D. A.; Chapman, K. T.; Bisaha, J. *J. Am. Chem. Soc.* **1984**, *106*, 4261–4263. (b) Evans, D. A.; Chapman, K. T.; Bisaha, J. *Tetrahedron Lett.* **1984**, *25*, 4071–4074. (c) Evans, D. A.; Chapman, K. T.; Hung, D. T.; Kawaguchi, A. T. *Angew. Chem., Int. Ed.* **1987**, *26*, 1184–1186. (d) Evans, D. A.; Chapman, K. T.; Bisaha, J. *J. Am. Chem. Soc.* **1988**, *110*, 1238–1256. (e) Evans, D. A.; Brown Ripin, D. H.; Johnson, J. S.; Shaughnessy, E. A. *Angew. Chem., Int. Ed.* **1997**, *36*, 2119–2121.
- (25) Evans, D. A.; Bartroli, J.; Shih, T. L. *J. Am. Chem. Soc.* **1981**, *103*, 2127–2129.
- (26) Evans, D. A.; Ennis, M. D.; Mathre, D. J. *J. Am. Chem. Soc.* **1982**, *104*, 1737–1739.
- (27) Evans, D. A.; Morrissey, M. M.; Dorow, R. L. *J. Am. Chem. Soc.* **1985**, *107*, 4346–4348.
- (28) Evans, D. A.; Britton, T. C.; Dorow, R. L.; Dellaria, J. F. *J. Am. Chem. Soc.* **1986**, *108*, 6395–6397.
- (29) Le Coz, S.; Mann, A. *Synth. Commun.* **1993**, *23*, 165–171.
- (30) Abdel-Magid, A.; Pridgen, L. N.; Eggleston, D. S.; Lantos, I. *J. Am. Chem. Soc.* **1986**, *108*, 4595–4602.
- (31) Caddick, S.; Jenkins, K.; Treweeke, N.; Candeias, S. X.; Afonso, C. A. M. *Tetrahedron Lett.* **1998**, *39*, 2203–2206.
- (32) (a) Lee, C.; Yang, W.; Parr, R. G. *Phys. Rev. B* **1988**, *37*, 785–789. (b) Becke, A. D. *J. Chem. Phys.* **1993**, *98*, 1372–1377. (c) Becke, A. D. *J. Chem. Phys.* **1993**, *98*, 5648–5652.
- (33) Hay, P. J.; Wadt, W. R. *J. Chem. Phys.* **1985**, *82*, 270–283. 299–310.
- (34) Gonzalez, C.; Schlegel, H. B. *J. Chem. Phys.* **1989**, *90*, 2154–2161. (b) Gonzalez, C.; Schlegel, H. B. *J. Phys. Chem.* **1990**, *94*, 5523–5527.